

SURFACE PLASMON SENSOR BASED ON POLYPYRROLE MULTIWALLED CARBON NANOTUBE COMPOSITE LAYER TO DETECT Al (III) IN AQUEOUS SOLUTION

A. BAHRAMI^a, A. R. SADROLHOSSEINI^b, G. MAMDOOHI^{c*},
K. BAHZAD^d, M. M ABDI^e

^aFaculty of Science, Department of Physics, Islamshahr Branch, Islamic Azad University, Islamshahr, Iran

^bCenter of Excellence for Wireless and Photonics Networks (WiPNet), Faculty of Engineering, Universiti Putra Malaysia, 43400UPM Serdang, Malaysia

^cQuantum & Laser Sciences (QLS) Group, Department of Physics, Faculty of Science, University of Malaya, 50603 Kuala Lumpur, Malaysia

^dFaculty of Science, Department of Physics, Shahr-e-Qods Branch, Islamic Azad University, Tehran, Iran

^eDepartment of Chemistry, Faculty of Science and Institute of Tropical Forestry and Forest Products, Universiti Putra Malaysia, Serdang, Selangor, Malaysia

In this study, the concentration of aluminum ion was measured using the surface plasmon resonance technique with polypyrrole multi-walled carbon nanotube composite layer and polypyrrole chitosan layer. The experiments were carried out at room temperature. The results of the measurement of the concentration of aluminum ion with polypyrrole multi-walled carbon nanotube layer were compared with that of the concentration of aluminum ion with polypyrrole chitosan layer. The angle shift for the polypyrrole multi-walled carbon nanotube composite layer was larger than the angle shift of the polypyrrole chitosan layer. The limitation of sensors was about 0.1 ppm.

(Received February 14, 2015; Accepted May 20, 2015)

Keyword: SPR sensor, Multi-walled carbon nanotube, PPy-CHI, Al ion

1. Introduction

Surface plasmon resonance (SPR) is a powerful technique to retrieve information on the optical properties of the biomaterials and nanomaterials. The Biosensor based on the SPR is a versatile method for the biological analysis. Essentially, the SPR depends on the optical properties of the metal layer [1] and the environmental changes. The SPR phenomenon is related to charge density oscillation at the interface between the layer and the ions solution or biomolecule [2]. Hence, the biomolecule is excessively sensitive to the plasmon resonance, removing the requirement for extrinsic biomolecule labeling [3]. One advantage of the SPR method is that the light beam never passes through the dielectric medium of interest; hence, the effect of absorbing the light in the analyte does not appear. Therefore, characterization of the medium after the metal layer and monitoring the interaction of the biomolecule with a sensing layer are the primary potentialities of the SPR.

Nanostructures have sparked interests in biosensing owing to their novelty and having unique properties. Different types of nanostructure-based biosensors include carbon nanotube, SnO₂ nanoparticles, nanowires, and gold nanoparticle. Nanostructure have contributed to improving the sensitivity, the selectivity, and the multiplexing capacity in the biosensors.

*Corresponding author: mahnaz@upm.edu.my

The SPR sensor is classified to angular, phase, intensity and polarization modulations. The SPR affinity biosensor is typically based on the angular modulation, and the output of the sensor is the resonance angle shift. When the sensor senses the biomolecules having low molecular weights or being in low concentrations, there will be a rise in the sensitivity of the sensor because the variation of the angle of the resonance is very small and detecting the molecules is daunting [4]. Accordingly, some researchers have used the nanoparticles and nanotubes (carbon nanotube) to enhance the angle shift and the sensor's sensitivity.

Carbon nanotubes (CNTs) have been used as both electrode and transducer components in biosensors for their interesting electrochemical and electrical properties including their flexibility to vary the electrical property (from metallic to semiconductor), small diameters, high mechanical strength, and easy fabrication integration. Wang [5] and Balasubramanian and Burghard [6] presented the design methodologies, performance characteristics, and potential applications of CNT biosensors, as well as the factors limiting their practical applications. It is obvious that many challenges still remain, especially in the sensitivity of the nanotube response to the environmental effects, and thus to the chosen type of the raw CNT material as well as its functionalization.

In recent years, various researchers have reported the properties of polypyrrole (PPy) based on humidity sensors [7-9] and gas sensors [10-12]. The conductivity of PPy has been observed to be higher than the other polymers. Moreover, the environmental stability and quick response recovery properties of PPy outweigh some inorganic materials [13-14].

Numerous methods such as atomic absorption spectroscopy, inductively coupled plasma-mass spectrometry (ICP-MS), and fluorescence spectrometry have been employed to detect and measure the concentration of metal and aluminum (Al) ions. The disadvantages of these methods include the experiment costs, the device costs, and the nonlinear calibration curve with each experiment. The explanation and carried out experiments require the chemical knowledge. Moreover, these methods do not have portability.

In this paper, Polypyrrole Multiwalled Carbon Nanotubes (PPy-MWCNT) composite layer was prepared by electro-polymerization of pyrrole (Py) and carbon nanotube. The PPy-MWCNT sensing layer incorporated with SPR was used to detect the Al (III), while the sensitivity and resonance angle shift were compared with the sensor based on polypyrrole chitosan (PPy-CHI) sensing layer.

2. Materials and methods

2.1 Preparation of PPy-MWCNT sensing layer

The preparation of PPy-MWCNT was explained in [15-16]. Briefly, the gold layer was coated on a microscope glass slide using the sputtering coater prior to coat the PPy-MWCNT or PPy-CHI. The thickness of the gold layer was 49 nm.

Multi-walled carbon nanotubes (Nanostructure & Amorphous Materials) and sodium dodecylbenzenesulfonate of analytical grade were purchased from Sigma-Aldrich. The outside and inside diameters of the MWCNT were 8 to 15 nm and 3 to 5 nm, respectively. The length and purity of the carbon nanotubes were 10 to 50 μm and >95 %, respectively.

The PPy-MWCNTs layer were synthesized by electrochemical (Autolab PGSTAT 101) polymerization of pre-distilled pyrrole on the MWCNT at the presence of sodium dodecylbenzenesulfonate (SDBS) in distilled water at room temperature. The weight ratio of the MWCNT to the pyrrole monomer was 0.7% which were dispersed in a SDBS solution, and the ratio of nanotubes to SDBS was 1:10. The pyrrole was dissolved in the MWCNT/SDBS solution and stirred. The Pyrrole-MWCNT premixed solution was electropolymerized at +0.7 V for 5 sec. The gold coated glass was used as a working electrode. A graphite rod and a saturated calomel electrode were used as the counter and reference electrode, respectively. The final PPy-MWCNT thin layer was washed with water and methanol with the aim of removing the electrolyte solution and dried under a vacuum at room temperature for 24 h [16].

2.2 Preparation of PPy-CHI sensing layer

The PPy-CHI sensing layer was coated on a gold layer by the electrochemical (Autolab PGSTAT 101) deposition method. The anodic potential of the working electrode was 1.1V relative to a saturated calomel electrode. The polymers were potentiostatically prepared in a solution containing 0.3M pyrrole (predistilled), 0.1M PTS dopant, and 0.7% w/v of CHI in acetic acid at room temperature [17].

2.3 SPR setup

As displayed in Figure 1, the SPR setup is based on Kretschmann configuration. It consists of a He-Ne laser (632.8 nm), a high index prism ($n=1.83956$, SF52), a precision rotation stage, a polarizer, a photodiode, a chopper and a flow cell [18]. The detailed explanation of Kretschmann configuration can be found elsewhere [19-20]. The prism was placed on a rotation stage and rotated up to 33° at an increment of a 0.016° step size. The photodiode, which is sensitive to intensity, was connected to the lock in amplifier to register the SPR signal when the rotation stage was momentarily stopped. The experiment was repeated more than ten times for each sample and the angle of resonance was registered along with the time [15].

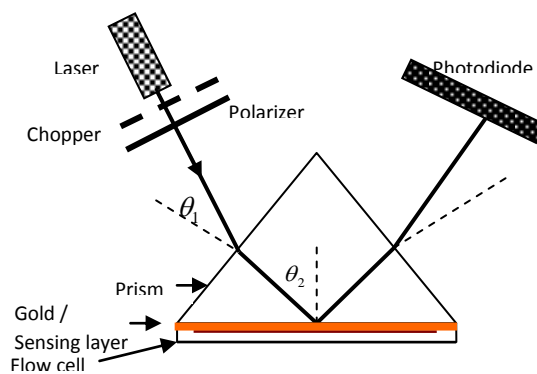


Fig. 1. The SPR setup includes laser, chopper, polarizer, prism, photodiode, and a flow cell.

The uncoated surface of the glass slide of the sensing unit was attached to the prism using an index matching gel. The DI water was first passed through the flow cell to be kept in direct contact with the sensing layer to determine the measurement base line. Once a stable base line was achieved, the setup and sensing layer were ready for measurement. Aqueous solutions of Al ions in different concentration were in turn passed through the flow cell separately. The sensing layer was expected to absorb the Al ions, and it could be detected by the SPR signal due to the change in the refractive index of the sensing layer and the thickness of the bound ion on its surface [21-22]. The Fresnel equation based on matrix method was used [22] for the data analysis with a computer program.

2.4 Ions solution

In the preparation of Al ions in aqueous solution, 1 g of aluminum nitrate was dissolved in 1l of deionized water (DI) separately, which resulted in a 1000 ppm Al (III) solution. Then, other concentrations (0.1, 0.5, 1, 5, 15, 25, 50, and 100 ppm) were prepared by systematic dilution of the 1000 ppm aluminum nitrate solution in DI water.

3. Results and Discussions

3.1 Calibration of SPR sensor

Fig. 2 displays the SPR signals of Prism/Gold layer/PPy-CHI/water and Prism/Gold layer/PPy-MWCNT/water configurations to determine the baseline. The experimental signals were fitted well to the theoretical the SPR reflectance signals.

$$R = rr^* , \quad (1)$$

where r denotes the reflection coefficient [17, 21-22]. The SPR signal is a function of the resonance angle, the refractive index of layer, and the refractive index of the interest medium (water); hence, the resonance angles were achieved by minimizing the summation of the difference value of the theory and the experimental reflectivity as follows:

$$T = \sum [R_{EXP} - R_{Theory}] , \quad (2)$$

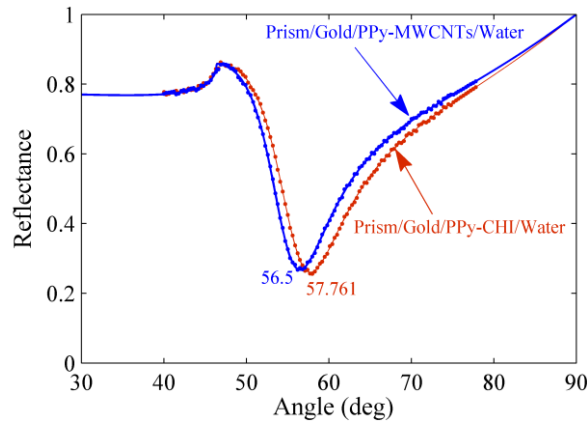


Fig. 2. SPR signals to determine the baseline

where R_{Exp} and R_{Theory} are the experimental and theoretical reflectivity. The angles of the resonance for Prism/ Gold layer/PPy-MWNT/water and Prism/ Gold layer/PPy-CHI/water configurations at the baseline were 56.5° and 57.761° , respectively.

3.2 Sensing of Al ion

In this experiment, the Al ion solution in different concentrations was separately loaded to the flow cell. The ion solution contacted the sensing layer (PPy-MWCNTs layer or PPy-CHI layer) during the 800 seconds. The SPR signal was recorded at different times using the computer program; the experiment was repeated more the 10 times for each sample. The angles of the resonance were obtained via the Eq (2). The angle shift was calculated from subtracting the resonance angle of baseline and the resonance angle of each experiment at different time. Figures 2(a) and 2(b) exhibit the variations of the angle shift versus time for the PPy-MWCNT sensing layer and the PPy-CHI sensing layer in different concentrations of Al ions in the aqueous solution. The angle shift increased with increasing the time until 500 s and after that the angle shift remained almost constant; this was the saturation value of the angle shift. The stars points were the experimental results that fitted well to Langmuire's first order adsorption model as follows [22-23].

$$\Delta\theta = \Delta\theta_{sat} (1 - \exp(-k_a t)) , \quad (3)$$

where $\Delta\theta$, $\Delta\theta_{sat}$, k_a and t are the angle shift, the saturated value of the resonance angle shift, the rate constant, and the response time of the sensor, respectively.

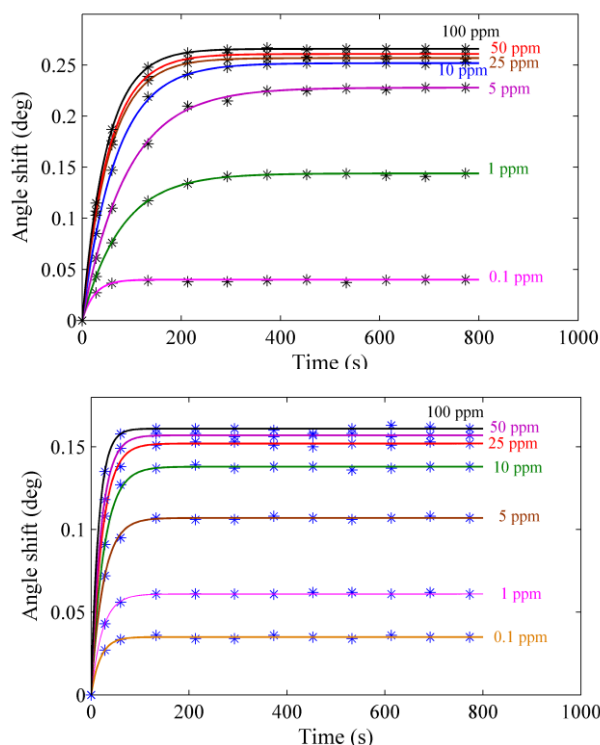


Fig. 3. The sensogram related to (a) PPy-MWCNTs sensing layer and (b) PPy-CHI sensing layer.

The variations of the saturated values of the angle shift with concentrations of the ions have been illuminated in Figure 4 for the PPy-MWCNTs and the PPy-CHI sensing layers. The experimental value was fitted to the Langmuir equation [15, 17, 23-24]. If $\Delta\theta_{\max}$, C , and K are the maximum value of the resonance angle shift, the concentration of the ions, and the affinity constant, respectively, the Langmuir equation is

$$\Delta\theta = \frac{\Delta\theta_{\max} C}{1/K + C}. \quad (4)$$

The experimental values were fitted to the theory with correlation coefficients greater than 0.96. Moreover, the variation of the PPy-MWCNTs sensing layer were larger than that of the PPy-CHI sensing layer. As a result, the sensitivity of the PPy-MWCNTs sensing layer to detect Al ion was higher than the PPy-CHI sensing layer.

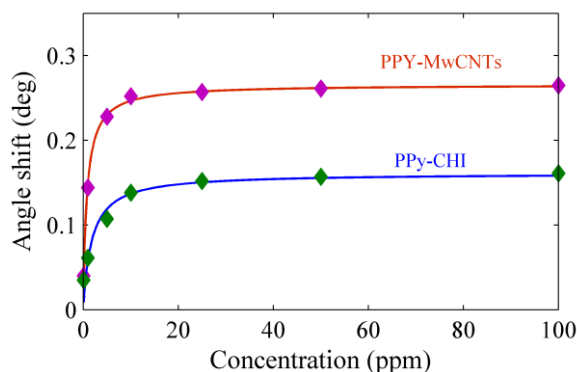


Fig. 4. Variation of the angle shift at the saturated value versus the concentration of Al ion.

The concentrations of the aqueous solution were measured using AAS before and after the experiments. Moreover, after the experiments, each sensing layer was immersed in DI water for 5 minutes to release the Al ion and the concentration of Al ion was measured using AAS. The obtained results are presented in Table 1.

Table 1 Al ion and the concentration of Al ion measurement using AAS

| Concentration of Al ion before the experiment (ppm) | Concentration of Al ion after the experiment (ppm) | Concentration of Al ion released form the layer in DI water (ppm) |
|---|--|---|
| 0.1 | 0.02 | 0.08 |
| 1 | 0.07 | 0.97 |
| 5 | 0.06 | 4.94 |
| 10 | 0.07 | 9.3 |
| 25 | 0.09 | 24.91 |
| 50 | 0.08 | 49.92 |
| 100 | 0.05 | 99.95 |

4. Conclusion

The SPR method is an accurate method for measuring the concentration of Al ion in the aqueous solution based on conductive polymers such as the PPy-MWCNT and PPy-CHI sensing layers. The sensitivity of the PPy-MWCNT was observed to be higher than PPy-CHI while the variation of the angle shift in low concentration of Al ion was linear.

Acknowledgment

The authors would like to acknowledge the Universiti Putra Malaysia (UPM) for funding this project under research grants, RUGS (Project No:05-02-122182RU).

References

- [1] O. Rengevich, *et al.*, *Semicond. Phys. Quantum Electron.* **2**, 28 (1999).
- [2] N. Peyghambarian, *et al.*, *Introduction to semiconductor optics*, (Prentice-Hall, Inc., 1994), pp 44-56.
- [3] A. R. Sadrolhosseini, *et al.*, Kim KY, *Plsmonics-Principles and Applications*, 253 (2012).
- [4] W. Hu, *et al.*, *Biosens. Bioelectron.* **19**, 1465 (2004).
- [5] J. Wang, *Electroanal.* **17**, 7 (2005).
- [6] K. Balasubramanian, M. Burghard, *Anal. Bioanal Chem.* **385**, 452 (2006).
- [7] A. Sun, *et al.*, *Sens. Actuators, B: Chem.* **142**, 197 (2009).
- [8] M. Alvarado, *et al.*, "Optical humidity sensor using Polypyrrole (PPy)," in *SPIE OPTO*, **7**, 825716 (2012).
- [9] R. Nohria, *et al.*, "Development of Humidity Sensors using Layer-by-Layer nanoAssembly of Polypyrrole," in *MRS Proceedings*, **4**, j16 (2005).
- [10] K. H. Kate, *et al.*, *J. Nanosci. Nanotech.* **11**, 7863 (2011).
- [11] K. Potje-Kamloth, *Crit. Rev. Anal. Chem.* **32**, 121 (2002).
- [12] S. C. Hernandez, *et al.*, *Electroanal.* **19**, 2125 (2007).
- [13] M. M. Abdi, *et al.*, *J. Mater. Sci.* **44**, 3682 (2009).
- [14] J. C. Yu, *et al.*, *Sens. Actuators, B: Chem.*, **101**, 236 (2004).

- [15] A. R. Sadrolhosseini, *et al.*, PloS one, **9**, e93962 (2014).
- [16] A. Bahrami, *et al.*, Adv. Mater. Res. **364**, 50 (2012).
- [17] A. R. Sadrolhosseini, *et al.*, Opt. Rev **18**, 331 (2011).
- [18] A. R. Sadrolhosseini, *et al.*, *International J. Polym. Mater. Polym. Biomater.*, **62**, 284 (2013).
- [19] M. M. Abdi, *et al.*, doi: 10.1371/journal.pone.0024578 (2011).
- [20] A. R. Sadrolhosseini, *et al.*, ARPN: J. Eng. Appl. Sci., **5**, 54 (2010).
- [21] J. Homola, Surf. Plasmon Resonan. Sens. **4**, 45 (2006).
- [22] R. B. Schasfoort and A. J. Tudos, Handbook of surface plasmon resonance, (Royal Society of Chemistry, 2008).
- [23] S. Chah, *et al.*, Sens. Actuators, B: Chem. **99**, 216 (2004).
- [24] E. S. Forzani, *et al.*, Environ. Sci. Technol. **39**, 1257 (2005).